

# Identification of Chemotaxis Parameters Using Microchannel for Bioremediation Applications

Marjan Khatami<sup>1</sup>, Zhi Chen<sup>1</sup>

Concordia University

1455 Boulevard de Maisonneuve O, Montréal, Canada

m\_khata@encs.concordia.ca; zhi.chen@concordia.ca

**Abstract** - Chemotaxis is the ability of bacteria to sense chemical concentration gradients in their environment and selectively migrate to chemical concentrations. By enhancing bacterial mixing within contaminated sites, this mechanism may enhance the efficiency of groundwater remediation technologies. Chemotaxis phenomena are complex in nature, and their effectiveness depends on the chemotactic sensitivity and the chemotactic receptor constant which depends on both the chemical attractant and the bacterial type. In this study we investigate the applicability of machine learning method for identification of chemotaxis parameters. To this end first a simplified mathematical model of the chemotaxis behaviour for a microchannel is extracted and it studied using both simulation software and numerical results. The synthetic data from simulation is then used for training a neural network with bacterial concentration along the microchannel as the input and two chemotaxis parameters as the outputs. The result of our study shows the suitable performance of the machine learning methods for identification of the chemotaxis parameters.

**Keywords:** Bioremediation, Chemotaxis, Bacterial population, Chemical attractant

## 1. Introduction

In bioremediation, living organisms are used to break down contaminants, particularly petroleum hydrocarbons, in the presence of ideal environmental conditions and sufficient nutrients. The process involves degrading or detoxifying substances hazardous to human health or the environment by utilizing naturally occurring bacteria and fungi or by using plants. Microbial metabolism is now considered a better, safer, and less expensive method for pollutant abatement than physicochemical methods. Chemotaxis is the ability of bacteria to sense chemical concentration gradients in their environment and selectively migrate to chemical concentrations [1]. The process of chemotaxis plays an important role in many physiological processes, including cancer metastasis, wound healing, embryogenesis, tissue morphogenesis, and so on [2, 3]. By enhancing bacterial mixing within contaminated sites, this mechanism may enhance the efficiency of groundwater remediation technologies. Many types of native soil-inhabiting bacteria exhibit chemotaxis toward common environmental pollutants. The chemosensory pathways and genes of different bacterial species are different, but chemotaxis as a whole is almost the same across species [4]. Bacteria show pathogenicity and symbiosis through chemotaxis to maintain an optimal niche in the environment. In addition to seeking food, bacteria use chemotaxis to survive in a constantly changing environment [5]. Bacteria consume simple sugars and/or amino acids as their source of energy. Chemotaxis uses these chemicals to move toward the food source by performing random walks and biased walks. Bacteria respond positively to the chemoattractants (attractants) and negatively to chemorepellents (repellents). Flagellar rotation is responsible for chemotaxis, which is a response to molecules that are sensed by the receptors within the flagella.

Chemotaxis phenomena are complex in nature, and their effectiveness depends on the chemotactic sensitivity and the chemotactic receptor constant, which depends on both the chemical attractant and the bacterial type [3]. The knowledge of these parameters helps for the efficient design of the bioremediation process using living organisms [3]. To this end, first, we first discuss the governing equations of chemotaxis phenomena. Chemotaxis is described by a set of coupled partial differential equations, which represents the concentration of bacterial populations in the presence of chemical attractants in three dimensions as a function of time [4]. For the identification of chemotaxis parameters, we consider a microchannel with a bacterial population at one end and a chemical attractant at the other end. For such a microchannel, the governing equations for the chemotaxis can be simplified in one-dimensional form. To this end, we extract the simplified equation and carry out a thorough analysis of the effect of chemotactic sensitivity and the chemotactic receptor constant on the distribution of the bacterial population in steady state for the certain concentrations of the chemical attractant and bacterial

population. Additionally, we have also developed a digital twin of the microchannel in COMSOL Multiphysics software to simulate the bacterial distribution through time and position along the microchannel. For the validation of the COMSOL model, the steady-state response of the simulated model is compared with that of the mathematical model, showing consistency in the results.

We also investigate the possibility of artificial neural networks for the identification of chemotaxis parameters through synthetic data obtained from the mathematical model. By considering the mathematical model as a substitute for the experimental setup, thousands of simulations are done for various combinations of chemotaxis sensitivity and chemotactic receptor constant, and the concentration of bacterial population within a microchannel is obtained. The data for the concentration of the bacterial population is considered as the input of the neural networks, and the normalized chemotactic sensitivity and chemotactic receptor constant are considered as the output of the network. The result of our study shows that neural networks can be a strong candidate for chemotactic parameter identification.

## 2. Chemotaxis modelling

The chemotactic phenomena are governed via two diffusion partial differential equations. The diffusion equation is a partial differential equation that describes density fluctuations in a material undergoing diffusion. Diffusion equations are used to model changes in concentration of a quantity of interest inside a specified region with respect to spatial and temporal variables [6]. The equation can be written as:

$$\frac{\partial \phi(\mathbf{r}, t)}{\partial t} = \nabla \cdot [D(\phi, t) \nabla \phi(\mathbf{r}, t)] + R_i \quad (1)$$

where  $\phi(\mathbf{r}, t)$  is the density of the diffusing material at location  $r$  and time  $t$  and  $D(\phi, \mathbf{r})$  is the collective diffusion coefficient for density  $\phi$  at location  $r$ ,  $\nabla$  represents the vector differential operator, and  $R_i$  is the effects of biological sources/sinks. If the diffusion coefficient depends on the density, then the equation is nonlinear, otherwise it is linear. Equation (4) describes the diffusion in three-dimensional space through time. When dealing with microchannels, it can be simplified in a one-dimensional form. The one-dimensional form the diffusion equation is given by:

$$\frac{\partial \phi}{\partial t} = D \frac{\partial^2 \phi}{\partial^2 x} + R_i \quad (2)$$

The solution of the above equation requires knowledge of the boundary condition. For a microchannel with a chemical attractant at one boundary and a bacterial population at the other end, the boundary conditions for the concentration profile in time and space,  $\phi(x, t)$ , are  $\phi(0, t) = \phi_o$  and  $\phi(L, t) = \phi_l$ , where  $L$  is the maximum length, and  $\phi_o$  and  $\phi_l$  are known values for both attractant and bacteria; the initial condition is  $\phi(x, 0) = 0$ .

Considering the general form of the diffusion equation in a one-dimensional form, the concentration of the chemical attractant  $a$  can be represented using the following equation:

$$\frac{\partial a}{\partial t} = D_a \frac{\partial^2 a}{\partial^2 x} \quad (3)$$

Additionally, the concentration of the bacterial population  $b$  can be expressed via:

$$\frac{\partial b}{\partial t} = D_b \frac{\partial^2 b}{\partial^2 x} + R_i \quad (4)$$

in which  $R_i$  is found using the chemotactic activity of the bacterial population using:

$$R_i = -\frac{\partial}{\partial x} (v_{ch} b) \quad (5)$$

where  $v_{ch}$  is the directional migration of the bacterial population due chemotaxis that is calculated using the following relation [6]

$$v_{ch} = \frac{2v}{3} \tanh\left(\frac{K_c \chi_0}{2v(K_c + a)^2} \frac{\partial a}{\partial x}\right) \quad (6)$$

in which  $v$  is the swimming velocity of the bacteria,  $\chi_0$  is the chemotactic sensitivity, and  $K_c$  is the chemotactic receptor constant. Considering the above discussed equation, the governing equation of the chemotaxis, with the bacterial population at one side and chemical attractant at the other side can be represented in the following set of equations:

$$\begin{cases} \frac{\partial a}{\partial t} = D_a \frac{\partial^2 a}{\partial x^2} \\ \frac{\partial b}{\partial t} = D_b \frac{\partial^2 b}{\partial x^2} - \frac{\partial}{\partial x} (v_{ch} b) \\ v_{ch} = \frac{2v}{3} \tanh\left(\frac{K_c \chi_0}{2v(K_c + a)} \frac{\partial a}{\partial x}\right) \\ b(0, t) = b_0 \\ b(l, t) = 0 \\ a(0, t) = 0 \\ a(l, t) = a_0 \\ b(x, 0) = 0 \\ a(x, 0) = 0 \end{cases} \quad (7)$$

As is clear from the Eq. (7), chemotaxis is function of both time and position. For the steady state analysis, we consider the time derivatives of the concentrations to be zero for both bacterial population and chemical attractant. In this way we will have one equation for chemical attractant as:

$$\begin{cases} 0 = D_a \frac{d^2 a}{dx^2} \\ a(0, t) = 0 \\ a(l, t) = a_0 \end{cases} \quad (8)$$

from which:

$$a = a_0 \frac{x}{L} \quad (9)$$

Substituting (9) into (4) results:

$$\begin{cases} 0 = D_b \frac{d^2 b}{dx^2} - \frac{d}{dx} \left( \frac{2bv}{3} \tanh\left(\frac{LK_c a_0 \chi_0}{2v(LK_c + a_0 x)}\right) \right) \\ b(0, t) = b_0 \\ b(L, t) = 0 \end{cases} \quad (10)$$

### 3. Steady state simulation study

For simulation study we consider Chemotactic response of *P. putida* F1 which is 1 mm apart from a toluene source, where the required parameters are obtained from [8], summarized as the following table:

Table 1: Chemotaxis parameters for *P. putida*-toluene

$v$ [ $\mu\text{m/s}$ ]	$K_c$ [ $\text{mM}$ ]	$D_b$ [ $\text{m}^2/\text{s}$ ]	$D_a$ [ $\text{m}^2/\text{s}$ ]	$\chi$ [ $\text{m}^2/\text{s}$ ]
44	1	3.2e-10	9.5e-10	5e-10

Additionally, the length of the microchannel is  $L = 1.5 \text{ mm}$ , and the concentration of the *P. putida* F1 is  $1 \text{ mol/m}^3$ . The simulation study has been carried out for various concentrations of chemical attractant ranging from  $0.001 \text{ mol/m}^3$  to  $5 \text{ mol/m}^3$ , illustrated in Fig. 5.

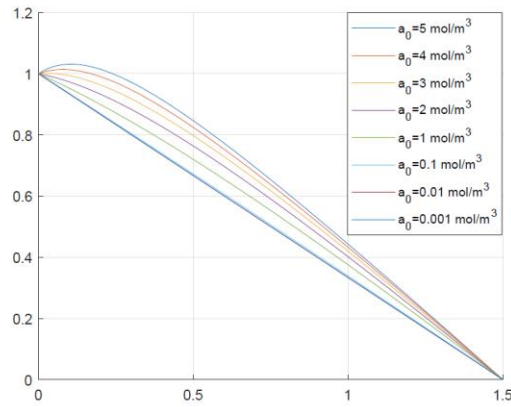


Figure 5: Chemotactic response of *P. putida* F1 in various concentrations of toluene

As it is clear from this figure, the distribution of *P. putida* F1 becomes linear for smaller toluene concentrations. To analyze the effect of chemotactic properties,  $K_c$ , and  $\chi_0$ . The chemotactic response with respect to various  $K_c$  is illustrated in Fig. 6, while other parameters are the same as in the previous study.

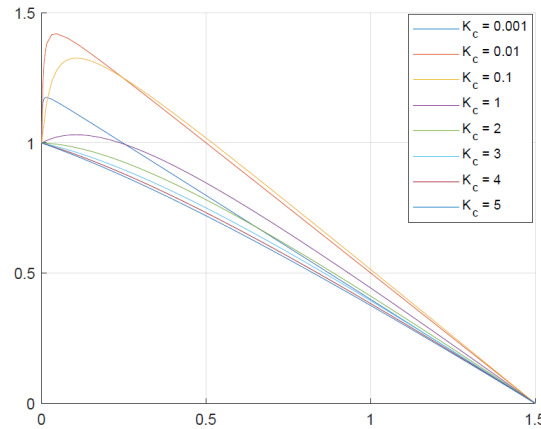


Figure 6: Effect of  $K_c$  on chemotactic response

As it can be seen from this figure, in the smaller value of  $K_c$  we observe the accumulation of the bacterial population at the source and increasing  $K_c$  leads to the linear distribution of the bacterial along the length. The chemotactic response with respect to  $\chi$  is illustrated in Fig. 7, with keeping the other parameters the same as in the previous study.

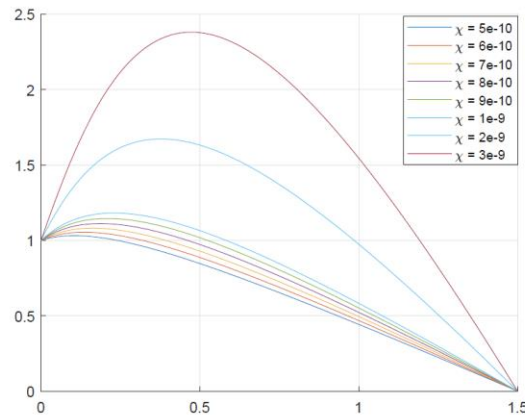


Figure 7: Effect of  $\chi_0$  on chemotactic response

As it is clear from this figure, increasing the  $\chi_0$  brings the bacterial concentration toward the center point.

#### 4. Time-dependant simulation study

For a thorough analysis of the chemotactic response of *P. putida* F1 in the presence of toluene, we developed a COMSOL model. This COMSOL model includes two “*Transport of Diluted Species*” modules, one for the bacteria and one for the chemical attractant. The simulated system is a miniaturized microfluidic system like the previous study, where the length of the microchannel is  $L = 1.5 \text{ mm}$ , and the concentration of the *P. putida* F1 is  $1 \text{ mol/m}^3$  and chemical attractant concentration of  $5 \text{ mol/m}^3$ .

Fig. 8 shows the distribution of the chemical attractant through time within the microchannel. As it is clear, it takes about 3000 s the have an even distribution of the chemical and the total amount of concentration increases through time.

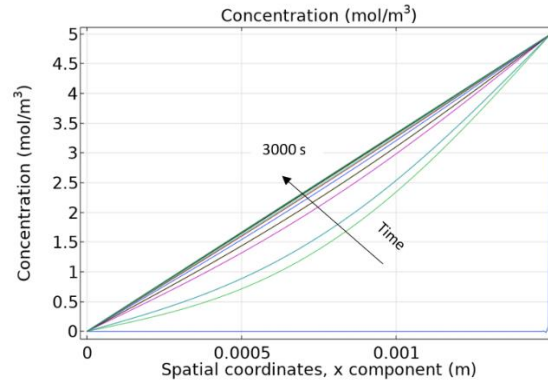


Figure 8: Chemical attractant concentration along the micro-channel

The distribution of the bacterial population is also depicted in Fig. 9. Referring to this figure, it is observed that the total distribution along the tube increases through time, and the accumulation of the bacteria is close to the source.

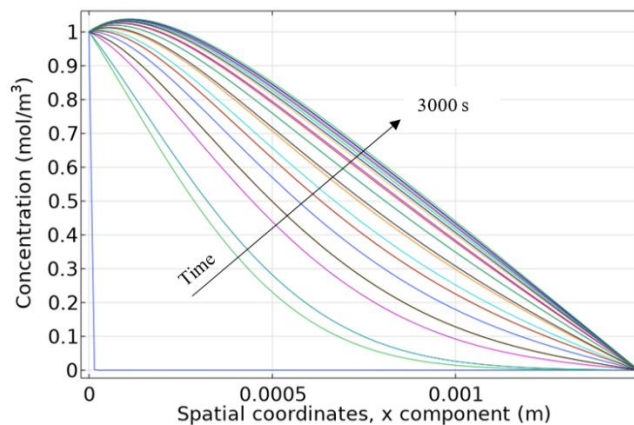


Figure 9: Bacterial population concentration along the micro-channel

#### 5. Parameter identification

The COMSOL model can work as a digital twin of the experimental setup and can be used as a reference to evaluate the proposed method for the identification of the chemotaxis phenomena.  $K_C$  and  $\chi_0$ . Fig. shows the results obtained from COMSOL and from the mathematical model for different  $K_C$   $\chi_0$ . Looking to the steady-state response of the Comsol model is observed that the maximum distribution of the bacterial population occurs at 0.1 mm along the channel with a maximum concentration of  $1.03 \text{ mol/m}^3$ . Comparing the result of the steady-state response from COMSOL with the reference plots (Figs. 7 and 8), it can be observed that the results best suit the chemotaxis response with  $K_C = 1 \text{ mol/m}^3$  and  $\chi_0 = 5e - 10$ .

Additionally, we have developed a neural network system with one hidden layer for identification of the chemotaxis parameters. The training of the network is done using synthetic data obtained from 1242 simulation with different values of  $\chi_0$  and  $K_c$  in the range of  $[0.1 \ 5]$  and  $[5 \ 30] e - 10$ . The input of the network is the concentration of the bacterial population in 20 different points along the tube in the steady state and the outputs are  $\chi_0$  and  $K_c$ . The performance of the designed neural network in identification of the chemotaxis parameters are depicted in Fig. 10, which shows a suitable performance.

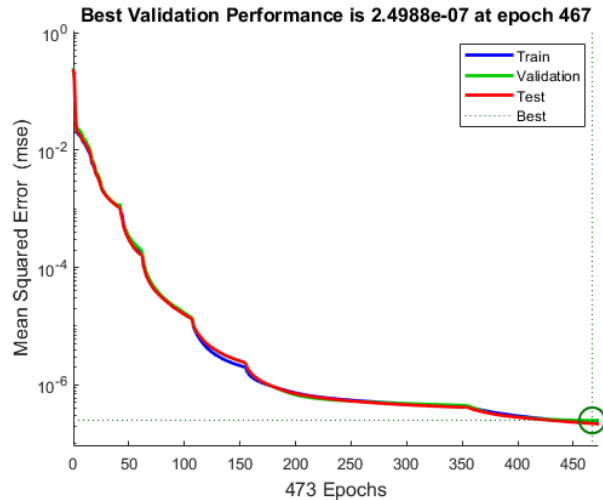


Figure 9: Performance of the neural network for estimation of chemotaxis parameters

#### 4. Conclusion

In this study we investigated the effects of chemotaxis parameters on distribution of the bacterial within a microchannel. The mathematical model of the chemotaxis behaviour was used to obtains synthetic data for training a neural network for identification of chemotaxis parameter. The result of the study shows the neural network is a promising solution for identification of chemotaxis parameters. This study can be enhanced via experimental data for future studies.

#### References

- [1] B. Klaus and P. Horn, Robot Vision. Cambridge, MA: MIT Press, 1986.
- [2] Dianqing Wu. Signaling mechanisms for regulation of chemotaxis. Cell research, 15(1):52–56, 2005.
- [3] Evanthia T Roussos, John S Condeelis, and Antonia Patsialou. Chemotaxis in cancer. Nature Reviews Cancer, 11(8):573–587, 2011
- [4] James A Hoch. Two-component and phosphorelay signal transduction. Current opinion in microbiology, 3(2):165–170, 2000.
- [5] George H Wadhams and Judith P Armitage. Making sense of it all: bacterial chemotaxis. Nature reviews Molecular cell biology, 5(12):1024–1037, 2004.
- [6] Xiang Jiang, Philip Cooper, and Paul J Scott. Freeform surface filtering using the diffusion equation. Proceedings of the Royal Society A: Mathematical, Physical and Engineering Sciences, 467(2127):841–859, 2011
- [7] Kevin C Chen, Peter T Cummings, and Roseanne M Ford. Perturbation expansion of alt’s cell balance equations reduce to segel’s one-dimensional equations for shallow chemoattractant gradients. SIAM Journal on Applied Mathematics, 59(1):35–57, 1998.
- [8] Xiaopu Wang, Tao Long, and Roseanne M Ford. Bacterial chemotaxis toward a napl source within a pore-scale microfluidic chamber. Biotechnology and bioengineering, 109(7):1622–1628, 2012.